

Short Communication

Investigation of Properties of Styrene-acrylic Copolymer containing Imidazole for Protection of HRB400 steel in Atmospheric Environment

Zhen Li

Jilin Province Economic Management Cadre College, College of Architectural Engineering, Jilin Changchun 130000, China

E-mail: teacher_73@126.com

Received: 23 November 2021 / *Accepted:* 18 January 2022 / *Published:* 4 March 2022

Styrene-acrylic copolymer is widely used in the anti-corrosion for construction. However, in the marine atmosphere for a long time, the corrosive medium diffuses to the metal surface through the interior of the paint system, resulting in serious corrosion of the metal. In this paper, the effects of imidazoline corrosion inhibitor added in styrene-acrylic copolymer for construction in atmospheric environment were studied by weightlessness experiment, image characterization and electrochemical test. The results showed that the overall corrosion rate of HRB400 metal matrix decreased exponentially with the increase of corrosion inhibitor contents. The obvious hole phenomenon on the surface of the paint gradually weakened and changed to the characteristics of stratification. The pitting corrosion of the metal substrate gradually changed to local corrosion, and the corrosion position was corresponding to the hole position of the paint. With the increase of corrosion inhibitor concentration, the corrosion potential increased, the corrosion current density decreased, while the double layer capacitance decreased and the charge transfer resistance increased. The effect of corrosion inhibitor added to the paint was mainly reflected in two aspects. On the one hand, imidazoline corrosion inhibitor can effectively promote cross-linking between macromolecules. On the other hand, imidazoline corrosion inhibitor was cationic, which can combine with anions and adsorb on metal surfaces instead of water molecules to inhibit corrosion.

Keywords: Styrene-acrylic copolymer; Imidazoline corrosion inhibitor; Improved paint; Atmospheric environment

1. INTRODUCTION

At present, the world's output of architectural paint is growing at an annual growth rate of 3.4%. Most of the external walls of buildings at home and abroad are decorated with architectural paint. As a

kind of exterior wall paint with special advantages, the styrene-acrylic copolymer is bound to show its unique style and obtain great development space in the field of architectural paint [1].

Styrene-acrylic copolymer is mainly composed of aggregate, binder and various auxiliary agents. The aggregate is mainly made of natural or artificial color sand (quartz composed of SiO_2). Aggregate grading determines the durability of styrene-acrylic copolymer. If the aggregate particle is coarse, it is easy to precipitate and pollution, while if too fine, its decorative effect will be greatly reduced. Acrylic emulsion is mostly used as adhesive material in styrene-acrylic copolymer, which plays a key role to determine the water resistance, stain resistance and bond strength of styrene-acrylic copolymer. Acrylic emulsion is mostly used as adhesive material in styrene-acrylic copolymer, which plays a key role to determine the water resistance, stain resistance and bond strength of styrene-acrylic copolymer. Auxiliaries are essential materials in styrene-acrylic copolymer, including film-forming auxiliaries, dispersants, defoaming agents, thickeners and other types. The film forming agents can increase the plastic of the film, the dispersants can promote the dispersion and mixing of aggregate, defoaming agents can inhibit bubble generation and to increase the compactness, and thickeners can make the construction of paint better, and can improve the stain resistance of styrene-acrylic copolymer.

In recent years, styrene-acrylic copolymer has become a shining star in building exterior wall coating, and it has developed most rapidly and actively in the field of paint. At present, most of the research on styrene-acrylic copolymer is about the construction process [2]. Morsch et al discussed the control points of paint in the exterior wall decoration of housing construction projects and the common problems of construction certificates combined with the case of a site project, and studied the key points of construction technology and quality control [3]. Alessi et al studied the factors affecting the color difference of paint [4]. Morsch et al studied the preparation process and formula modification of emulsion used in paint, so as to improve the durability of styrene-acrylic copolymer [5]. Linde et al analyzed the whitening problem of paint and proposed corresponding solutions [6].

The film forming mechanism of styrene-acrylic copolymer is the same as that of ordinary paint, which is the process of combining pigment particles and polymer particles into a whole. Styrene-acrylic copolymer protects the building metal by blocking and shielding the corrosive medium and blocking the corrosive current with high resistance. However, in the long-term operation process, due to the inevitable microscopic defects in the paint, when the paint surface is wetted and a certain amount of water passes through the coating, the soluble corrosive medium begins to dissolve [7-9]. The existence of the contents of osmotic pressure inside and outside the paint makes the corrosive medium penetrate into the coating along the pores. Due to the swelling of the water inside the paint, coupled with the process of water absorption and dehydration in the coating, resulting in internal stress, so the water absorption capacity of the paint can be used as a sign of corrosion resistance. When the internal stress is greater than the adhesion between the paint and the metal matrix, the formation of blisters, making the paint internal defects more and more, in which corrosion medium is easier to reach the metal matrix and then metal corrosion under the film occurs [10-12]. Therefore, in this paper, imidazoline corrosion inhibitor was added to modify and improve into styrene-acrylic copolymer, to meet the needs of marine atmospheric environment.

2. EXPERIMENTAL SETTINGS

HRB400 steel was used as the metal material for the test, and the main components were shown in Table 1.

Table 1. Main components of HRB400 steel (wt.%)

Element	C	Si	Mn	P	S	Ceq
Content	0.25	0.80	1.60	0.045	0.045	0.52

The HRB400 steel for exposed experiment in atmospheric environment was cleaned by acetone, deionized water and alcohol successively, and then dried for more than 24 h. The steel for electrochemical test was required to weld a wire on the back and then encapsulated by epoxy resin. The aggregate (composed of quartz in 10% for 20-40 mesh, 80% for 40-80 mesh, and 10% for 80-120 mesh) and imidazoline corrosion inhibitor (with the content of 0,10 g/L 30 g/L, 50 g/L, 70 g/L and 90 g/L, respectively) were added in styrene-acrylic emulsion to form the improved paint studied in this paper. The experimental paint was styrene-acrylic emulsion with or without imidazoline corrosion inhibitor in different contents. The paint was applied on the surface of the HRB400 steel (25×25 mm²) by hand brush and cured for 7 days at 20°C. The thickness of the samples set as 10±2 µm was determined by QNIX8500 gauge through five-point sampling method [13,14].

Different experimental samples were placed in the marine atmosphere for 30 days. After the experiment, the microscopic characteristics of the paint on the experimental surface were observed by SEM (scanning electron microscope). After removing the surface coating and corrosion products, the surface corrosion morphology was obtained after drying by Zeiss microscope, and then weighed and calculated the corrosion rate obtained by mass loss method.

After exposed in marine atmosphere for 30 days, the electrochemical tests of experimental samples were carried out in 3 wt.% NaCl solution at room temperature of about 20±1°C. The polarization curve was tested using a three-electrode system, in which the reference potential (RE) was saturated calomel electrode (SCE), the auxiliary electrode (AE) was platinum electrode (Pt), and the working electrode (WE) was coated HRB400 steel after exposed experiment in atmospheric environment. The electrochemical workstation used Princeton PARSTST 2273. When the open circuit potential (OCP) of the WE fluctuated within 300 s within ±10 mV, the polarization curve was tested. The scanning potential range was ±250 mV (vs.OCP), and the scanning rate was 0.01667 mV/s, while the frequency of electrochemical impedance spectrum (EIS) was set as 10⁵-10⁻² Hz with an AC disturbance voltage of 5 mV. ZSimpWin and PowerSuite software of the system were used for data analysis.

3. RESULTS AND DISCUSSION

3.1 Mass loss measurements

Figure 1 showed the corrosion rate of HRB400 steel after exposed to marine atmosphere for 30 days with different corrosion inhibitor contents. It can be seen from the figure that when no corrosion inhibitor was added to the paint, the corrosion rate reached 0.1245 mm/a, far higher than the acceptable

metal corrosion rate (less than 0.076 mm/a) [15]. With the increase of corrosion inhibitor content in the paint, the corrosion rate of HRB400 metal matrix decreased exponentially, that is, the corrosion rate decreased rapidly first and then slowly with the increase of corrosion inhibitor content. When the content of corrosion inhibitor was 50 g/L, the corrosion rate was 0.07655 mm/a, which can be approximately considered to meet the requirements of corrosion control. When the corrosion inhibitor content was 90 g/L, the corrosion rate was 0.06996 mm/a, in which the corrosion rate decreased slightly, only 1.65×10^{-4} (mm/a)/(g/L). Therefore, it can be deduced from the corrosion rate of HRB400 steel matrix that the addition of corrosion inhibitor can effectively reduce the metal corrosion rate caused by the diffusion of corrosive medium and paint failure, which proved the effectiveness of the improved paint proposed in this paper [16].

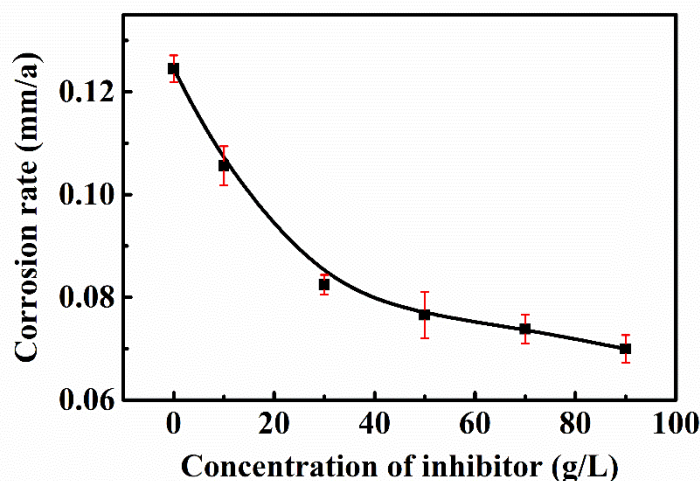


Figure 1. The corrosion rate obtained by mass loss method of HRB400 steel coated with paints under different corrosion inhibitor contents (0,10 g/L 30 g/L, 50 g/L, 70 g/L and 90 g/L, respectively) after exposed in marine atmosphere for 30 days

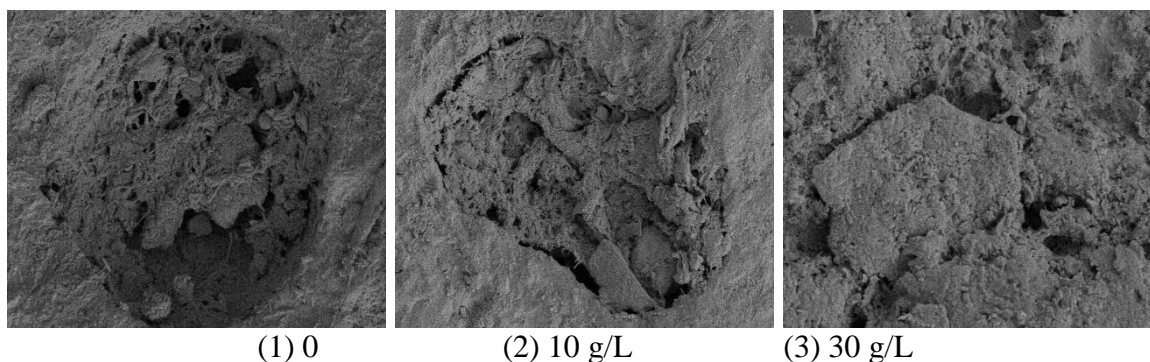
3.2 Corrosion morphology

Figure 2 showed the surface microscopic morphology of painted HRB400 samples exposed to marine atmosphere for 30 days with different corrosion inhibitor contents in paint. Figure 3 showed the corrosion morphology of the HRB400 metal matrix after removing the paint and surface corrosion products. As can be seen from the Figure 2, when no corrosion inhibitor was added to the paint, there was an obvious "collapse" pit on the surface of the paint after 30 days of exposure to the marine atmospheric environment. This was because water molecules diffused into the paint and destroyed the cross-linked macromolecules, resulting in obvious macroscopic damage on the paint surface. At this time, a large number of corrosive media reached the metal surface, causing corrosion of the metal matrix. As can be seen from Figure 3, when no corrosion inhibitor was added to the paint, the surface of the metal matrix showed obvious pitting characteristics [17-20]. This was because when the corrosive medium reached the paint/metal interface, due to the occluded characteristics of the interface, the oxygen contents cell with the external cathode and the interface as the anode was formed. At this time, the Fe^{2+}

generated by activation corrosion hydrolyzed ($\text{Fe}^{2+} + 2\text{H}_2\text{O} \rightarrow \text{Fe}(\text{OH})_2 + 2\text{H}^+$) and the interface acidified, resulting in obvious pitting of the metal matrix. At the same time, the dense corrosion product Fe_3O_4 generated at the interface covered the metal surface, and then the diffusion of Cl^- further promoted the pitting process of the matrix [21].

When different contents of corrosion inhibitor were added to the paint, it can be seen from Figure 2 that the obvious pitting phenomenon on the paint surface gradually decreased. When the content of corrosion inhibitor was 30 g/L, the paint surface no longer had obvious features of holes, but changed to layered features, and the paint surface still showed the fracture phenomenon of macromolecular chains. With the continuous increase of corrosion inhibitor content, the integrity of the paint surface was gradually enhanced, and the stratification phenomenon disappeared gradually. When the corrosion inhibitor content was 90 g/L, there were only a few tiny holes on the surface of the paint, and the general integrity of the paint was high [22,23]. As can be seen from Figure 3, with the increase of the contents of corrosion inhibitor added, the pitting characteristics of the metal matrix surface gradually weakened, and the corrosion gradually concentrated in local areas. When the contents of corrosion inhibitor for 50 g/L, the metal specimen surface can be divided into apparent corrosion area and no-corrosion area. As the inhibitor contents continued to increase, the corrosion area densely distributed in several areas. When the contents of corrosion inhibitor increased to 90 g/L, it can be seen that the corrosion area was mainly located in the middle part [24]. The field macroscopic experiment results showed that the corrosion area was mainly corresponding to the location of the tiny holes in Figure 2(6).

The effect of corrosion inhibitor added to the paint was mainly reflected in two aspects. On the one hand, imidazoline corrosion inhibitor was a macromolecule structure. When added to the paint, imidazoline corrosion inhibitor can effectively promote the cross-linking between macromolecules, block the diffusion channel, and improve the density of the system. On the other hand, imidazoline corrosion inhibitor was a cationic corrosion inhibitor, and the main anion that caused serious corrosion of metal matrix by diffusion to the coating/metal interface was anion [25]. Therefore, in the channel diffusion and at paint/metal interface, when anions reach the metal surface, anions and cationic corrosion inhibitors can effectively combine to reduce the damage of anions to the metal matrix, thus the amount of corrosion products generated was reduced, and then the interface expansion effect was reduced, so as to ensure the integrity of the paint [26].



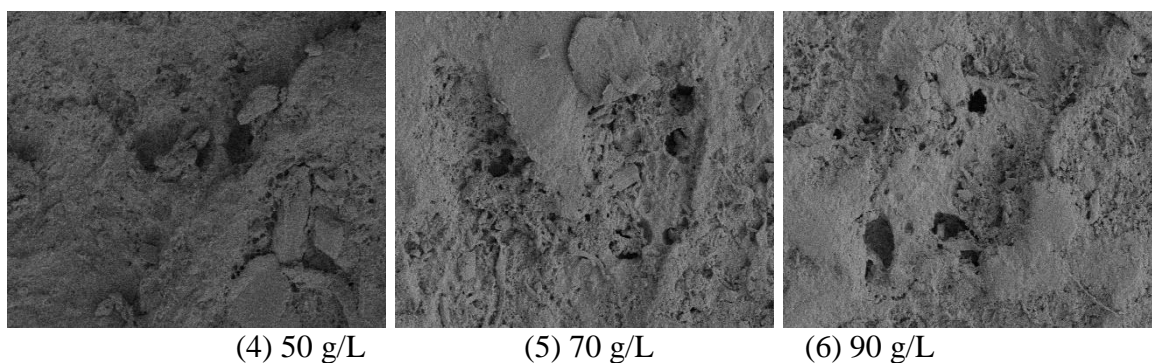


Figure 2. Corrosion morphology in precision of 50 μm of paint surface under different corrosion inhibitor contents (0,10 g/L 30 g/L, 50 g/L, 70 g/L and 90 g/L, respectively) after exposed in marine atmosphere for 30 days

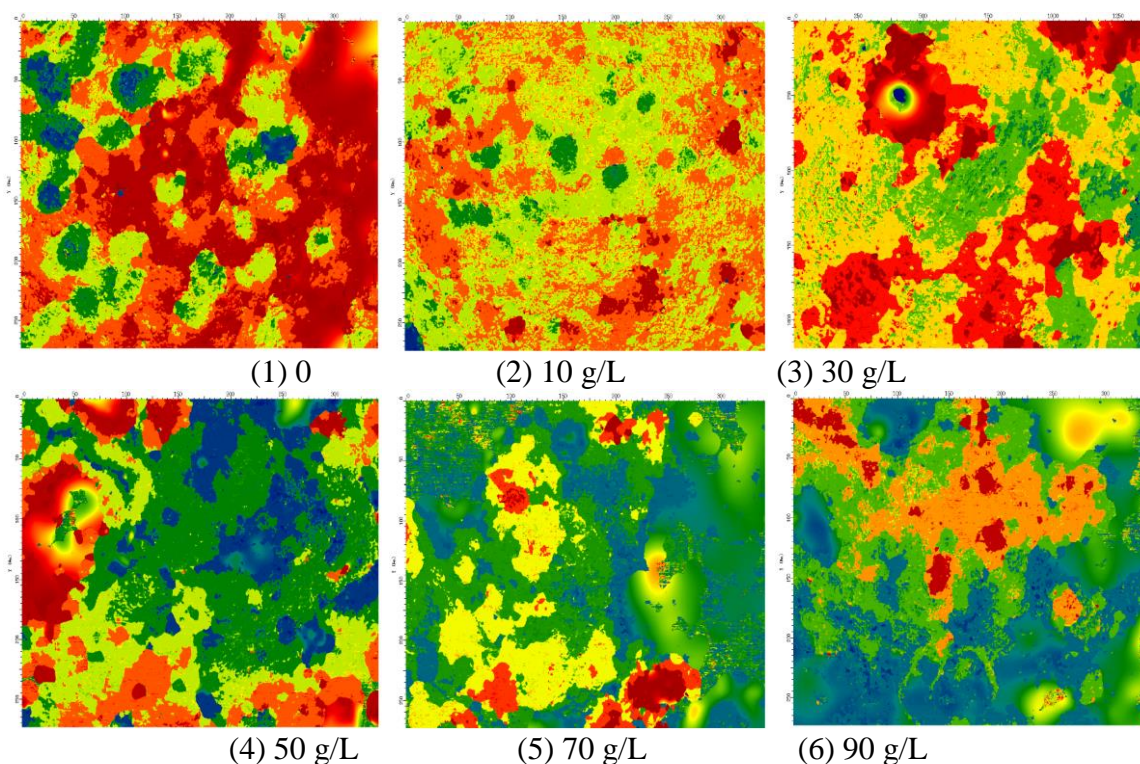


Figure 3. Corrosion morphology of HRB400 steel coated with paints under different corrosion inhibitor contents (0,10 g/L 30 g/L, 50 g/L, 70 g/L and 90 g/L, respectively) after exposed in marine atmosphere for 30 days

3.3 Electrochemical experiment

Electrochemical experiments were carried out on experimental samples with different corrosion inhibitors after 30 days of exposure in marine atmosphere. Polarization curves and electrochemical impedance curves were shown in Figure 4. The experimental medium was NaCl solution with a mass fraction of 3.5% and the experimental temperature was 25°C.

As can be seen from the figure of polarization curves, as the contents of corrosion inhibitor increased, the polarization curve moved toward the direction of potential increase and corrosion current decrease on the whole. When the corrosion potential increased, the corrosion resistance of the paint system increased [27]. When the corrosion current density decreased, the corrosion rate slowed down, and the corrosion inhibition efficiency of the inhibitor increased. For another aspect, the anode polarization curve changed obviously and the anode Tafel curve moved forward. Therefore, in this paper, the corrosion inhibitor was mainly adsorbing at the active site of the anode reaction to inhibit metal dissolution and reduced the corrosion current. Table 2 showed the fitting parameters of the polarization curve. With the increase of corrosion inhibitor content from 10 g/L to 90 g/L, the corrosion potential increased from -782.3 mV to -610.4 mV, and the inhibition efficiency increased from 62.90% at 10 g/L to 74.80% at 90 g/L. At the same time, the anode Tafel slope decreased gradually from 55.7 mV/dec to 38 mV/dec, and the positive deviation of corrosion potential of metals in the system at all contents was more than 100 mV, indicating that imidazoline corrosion inhibitor was anodic corrosion inhibitor, which mainly reduced corrosion current by inhibiting anodic dissolution of metals [28,29].

In the EIS curve, capacitive reactance arcs appeared in the high frequency zone, which was related to the charge transfer process on the metal surface. According to the characteristics of Nyquist diagram, the equivalent circuit was chosen as $R_s(Q(R_p(C_{dl}R_{ct})))$, in which R_s was solution resistance, Q was capacitance, R_p was corrosion resistance on metal surface (including corrosion product film, coating and corrosion inhibitor), C_{dl} was double electric layer capacitance, and R_{ct} was charge transfer resistance on metal substrate surface. The fitting results are shown in Table 3. As can be seen from Figure 4(2) and Table 3, the corrosion rates of the samples were different with the radius of capacitive reactance arc. The larger the radius of capacitive arc was, the smaller the corrosion rate was, and the higher the inhibition rate of corrosion inhibitor was. It can be seen that with the increase of the contents of corrosion inhibitor added, the radius of capacitive arc increased, indicating that the corrosion rate was smaller, which was the same as the result of corrosion current density [30].

In EIS curves, charge transfer resistance (R_{ct}) was generally used to evaluate the corrosion inhibition performance of corrosion inhibitor adsorption film on electrode surface. Without corrosion inhibitor, the R_{ct} was only $107.1 \Omega \cdot \text{cm}^2$. The R_{ct} increased with the addition of corrosion inhibitor, and gradually increased from $594 \Omega \cdot \text{cm}^2$ to $1208 \Omega \cdot \text{cm}^2$ with the increase of corrosion inhibitor contents from 10 g/L to 90 g/L, indicating that corrosion inhibitor was adsorbed on the metal surface, forming an adsorption layer, and increasing the resistance of electrode reaction process, thus the electrochemical corrosion process was inhibited [31]. The adsorption layer can prevent the diffusion of corrosive medium on the metal surface and play a role of corrosion inhibition. The R_{ct} increased with the increase of the content of corrosion inhibitor, that is, with the increase of the contents of corrosion inhibitor, the adsorption film on the metal surface became more dense or thicker, indicating that the diffusion effect of corrosion inhibitor film on the metal/solution interface was enhanced, resulting in better corrosion inhibition effect [32].

The double layer capacitance (C_{dl}) for paint with corrosion inhibitor was smaller than that of the sample without corrosion inhibitor under the same condition, because after the addition of corrosion inhibitor, the corrosion inhibitor molecule will replace the water molecule adsorbed on the surface of the metal matrix, physically or chemically adsorbed on the surface of the metal matrix [33]. In addition,

because the dielectric constant of water was relatively large and the thickness of the film formed by water molecules was usually smaller than that formed by the corrosion inhibitor molecules, the capacitance of the C_{dl} decreased after the addition of corrosion inhibitor. That is, after the addition of corrosion inhibitor, the interaction between corrosion inhibitor and metal was stronger than the interaction between water molecules and metal, corrosion inhibitor replaced the adsorbed water molecules and formed an adsorption film, and furthermore the dielectric constant of corrosion inhibitor with a large volume was small, so the double layer capacitance C_{dl} was reduced. This showed that the corrosion inhibitor film formed by the adsorption of corrosion inhibitor on the metal surface was dense, and the corrosion inhibition effect was further improved [34,35]. The law of corrosion inhibition obtained by impedance spectrum was in good agreement with that obtained by weight loss experiment and polarization curve.

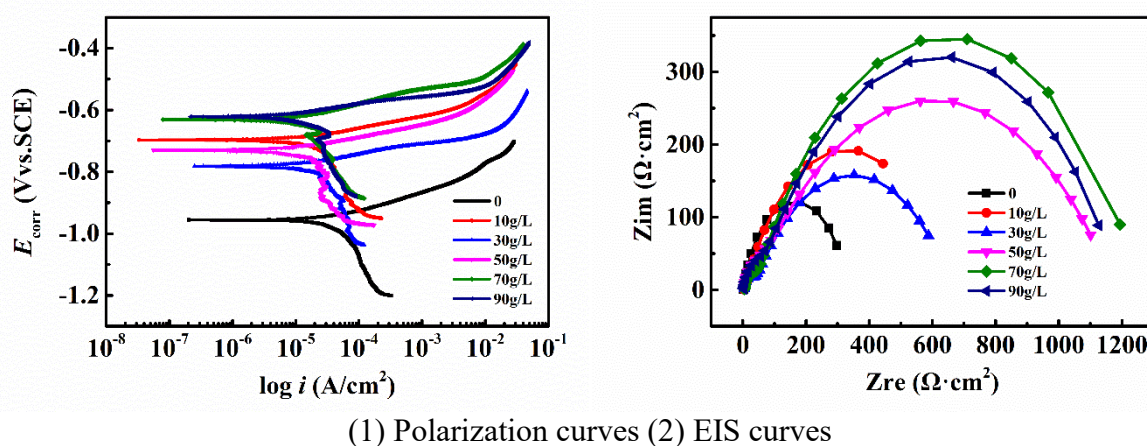


Figure 4. Experimental results of electrochemical testing including polarization curves and EIS curves of paint systems with different corrosion inhibitor contents (0,10 g/L 30 g/L, 50 g/L, 70 g/L and 90 g/L, respectively) in 3 wt.% NaCl solution at room temperature of about 20±1°C after exposed in marine atmosphere for 30 days

Table 2. Fitting results of polarization curves of paint systems with different corrosion inhibitor contents (0,10 g/L 30 g/L, 50 g/L, 70 g/L and 90 g/L, respectively) in 3 wt.% NaCl solution at room temperature of about 20±1°C after exposed in marine atmosphere for 30 days

Contents (g/L)	E_{corr} (mV vs. SCE)	I_{corr} ($\mu\text{A}/\text{cm}^2$)	β_a (mV/dec)	β_c (mV/dec)
0	-953	56	71	468
10	-782	21	56	665
30	-732	18	46	295
50	-701	19	44	288
70	-627	15	55	346
90	-610	14	38	304

Table 3. Fitting results of EIS curves of paint systems with different corrosion inhibitor contents (0,10 g/L, 30 g/L, 50 g/L, 70 g/L and 90 g/L, respectively) in 3 wt.% NaCl solution at room temperature of about $20\pm 1^\circ\text{C}$ after exposed in marine atmosphere for 30 days

Contents (mg/L)	$R_s (\Omega \cdot \text{cm}^2)$	$Q (\mu\text{F}/\text{cm}^2)$	n	$R_p (\Omega \cdot \text{cm}^2)$	$C_{dl} (\mu\text{F}/\text{cm}^2)$	$R_{ct} (\Omega \cdot \text{cm}^2)$
0	2.231	444.6	0.813	328.4	415.2	107.1
10	2.928	127.8	0.693	25.02	231.3	594.0
30	4.068	2.7	0.905	34.78	212.5	621.1
50	4.114	0.8	0.964	51.60	165.4	1113.6
70	4.936	5.5	0.882	45.38	143.4	1120.4
90	2.891	3.5	0.905	75.62	130.3	1208.3

4. CONCLUSION

In this paper, the effects of imidazoline corrosion inhibitor added in styrene-acrylic emulsion for construction in atmospheric environment were studied by weightlessness experiment, image characterization and electrochemical test. The main conclusions were as follows.

(1) The corrosion rate of HRB400 metal matrix decreased rapidly first and then slowly with the increase of corrosion inhibitor contents. When the added corrosion inhibitor contents was 50 g/L, the corrosion rate was 0.07655 mm/a, which can be approximately considered to meet the requirements of anti-corrosion (less than 0.076 mm/a).

(2) With the increase of corrosion inhibitor contents, the obvious pitting phenomenon on the surface of the paint gradually weakened and changed to the layered feature. When the corrosion inhibitor content was 70 g/L, the integrity of the coating surface was gradually enhanced and the layered phenomenon disappeared. The pitting corrosion of the metal substrate gradually changed to local corrosion, and the corrosion position was corresponding to the hole position of the paint.

(3) With the increase of the corrosion inhibitor contents, the corrosion potential increased and the corrosion current density decreased, indicating that the corrosion resistance of the coating system increased. In addition, the positive deviation of corrosion potential of the metals in the system at each content was more than 100 mV, indicating that the imidazoline corrosion inhibitor was anodic. At the same time, the double layer capacitance decreased while the charge transfer resistance increased, which was caused by the adsorption of corrosion inhibitor on the metal surface instead of water molecules.

References

1. S. An, M.W. Lee, A.L. Yarin and S.S. Yoon. *Chem. Eng. J.*, 344 (2018) 206.
2. A. Pathania, R.K. Arya and S. Ahuja. *Prog. Org. Coat.*, 105 (2017) 149.
3. S. Morsch, S. Lyon, P. Greensmith, P. Lyon and S. Morsch. *Prog. Org. Coat.*, 78 (2015) 293.
4. S. Alessi, E. Caponetti, O. Güven, M Akbulut, G. Spadaro and A. Spinella. *Macromol. Chem. Phys.*, 216 (2015) 538.
5. S. Morsch, S. Lyon, S.D. Smith and S.R. Gibbon. *Prog. Org. Coat.*, 86 (2015) 173.
6. E. Linde, N.H. Giron and M.C. Celina. *Polymer*, 153 (2018) 653.

7. C. Yang, X. Xing, Z.L. Li and S.X. Zhang. *Polymers-basel*, 12 (2020) 138.
8. G.M.A. El-Hafeez, M.M. El-Rabeie, A.F. Gaber and Z.R. Farag. *J. Coat. Technol. Res.*, 18 (2021) 581.
9. L.W. Ma, J.K. Wang, D.W. Zhang, Y. Huang, L.Y. Huang, P.J. Wang, H.C. Qian, X.G. Li, H.A. Terryn and J.M.C. Mole. *Chem. Eng. J.*, 404 (2021) 127118.
10. G. Bouvet, Nguyen Dang, S. Cohendoz, X. Feaugas and S. Touzain. *Prog. Org. Coat.*, 96 (2016) 32.
11. T. Miwa, Y. Takeshita, A. Ishii and T. Sawada. *Prog. Org. Coat.*, 120 (2018) 71.
12. S. Ghojavand, R. Arefinia and H. Sahrayi. *Prog. Org. Coat.*, 97 (2016) 301.
13. A. Yabuki and M. Kanagaki, C. Nishikawa, H.L. Ji and I.W. Fathona. *Prog. Org. Coat.*, 154 (2021) 106194.
14. J.D. Zuo, B.Q. Dong, F. Xing, C.Y. Luo, J. Zhan and L. Wang. *Power Technol.*, 389 (2021) 32.
15. T.F. Liu, W. Li, C.Y. Zhang, W. Wang, W.W. Dou and S.G. Chen. *J. Ind. Eng. Chem.*, 97 (2021) 560.
16. A. Suárez-Vega, C. Agustín-Sáenz, L. A. O'Dell, F. Brusciotti, A. Somers, M. Forsyth. *Appl. Surf. Sci.*, 561 (2021) 149881.
17. G. Bouvet, D. Trinh, S. Mallarino, X. Feaugas and S. Touzain. *Prog. Org. Coat.*, 96 (2016) 13.
18. A.S. Nguyen, N. Causse, M. Musiani, M.E. Orazem and V. Vivier. *Prog. Org. Coat.*, 112 (2017) 93.
19. W.F. Yang, W.B. Feng, Z.T. Liao, Y.P. Yang, G.L. Miao, B. Yu and X.W. Pei. *Surf. Coat. Tech.*, 406 (2021) 126639.
20. H. Yan, W. Li, H. Li, X.Q. Fan and M.H. Zhu. *Prog. Org. Coat.*, 135 (2019) 156.
21. P. Rahmani, A. Shojaei and N.P. Tavandashti. *J. Ind. Eng. Chem.*, 83 (2020) 153.
22. R. Kumar, K.K. Pandey, A. Islam and A.K. Keshri. *J. Alloy Compd.*, 809 (2019) 151819.
23. C. Araújo, I.L.S. Almeida, H.C. Rezende, S.M.L.O. Marcionilio, J.J.L. León and T.N. de Matos. *Microchem. J.*, 137 (2018) 348.
24. Z. Mahidashti, T. Shahrabi and B. Ramezanzadeh. *Prog. Org. Coat.*, 114 (2018) 19.
25. K. Vinothkumar, M. Nivetha and M.G. Sethuraman. *Iran. Polym. J.*, 29 (2020) 919.
26. J.K. Li, H.B. Zeng and J.L. Luo. *Chem. Eng. J.*, 421 (2021) 127752.
27. H. Lee, S. Yun, A. Al-Shishani, A.A. Rahim and B.R. Pandian. *Prog. Org. Coat.*, 135 (2019) 536.
28. M. Pecora, Y. Pannier, M.C. Lafarie-Frenot, M. Gigliotti and C. Guigon. *Polym. Test.*, 52 (2016) 209.
29. V. Dalmoro, D.S. Azambuja, C. Alemán and E. Armelin. *Surf. Coat. Tech.*, 357 (2019) 728.
30. S. Kumar, S.K. Samal, S. Mohanty and S.K. Nayak. *J. Therm. Anal. Calorim.*, 137 (2019) 1567.
31. C. Yang, Q. Han, A.Q. Wang, W. Han, L. Sun and L.S. Yang. *Des. Monomers Polym.*, 24 (2021) 73.
32. J. Yang, B. Carsten, S.V. Lamaka, S. Darya, X. Lu, S. Di and M.L. Zheludkevich. *Corros. Sci.*, 140 (2018) 99.
33. Y. Morozov, L.M. Calado, R.A. Shakoor, R. Raj, R. Kahraman, M.G. Taryba and M.F. Montemor. *Corros. Sci.*, 159 (2019) 108128.
34. S. Gangopadhyay and P.A. Mahanwar. *J. Coat. Technol. Res.*, 15 (2018) 789.
35. L.M. Calado, M.G. Taryba, Y. Morozov, M.J. Carmezim and M.F. Montemor. *Corros. Sci.*, 170 (2020) 108648.